

Mediterranean Marine Science

Vol 26, No 1 (2025)

Mediterranean Marine Science



Diatom distribution and long-term survival in a heavily polluted sediment core from the Bay of Bagnoli (Tyrrhenian Sea, Italy)

ANGELA PELUSI, MARÍA LORENA ROMERO MARTÍNEZ, APURVA MULE, ELEONORA SCALCO, INES BARRENECHEA ANGELES, ROBERTA PIREDDA, WIEBE KOOISTRA H.C.F. , MARINA MONTRESOR, DIANA SARNO

doi: [10.12681/mms.37946](https://doi.org/10.12681/mms.37946)

To cite this article:

PELUSI, A., ROMERO MARTÍNEZ, M. L., MULE, A., SCALCO, E., BARRENECHEA ANGELES, I., PIREDDA, R., KOOISTRA H.C.F. , W., MONTRESOR, M., & SARNO, D. (2025). Diatom distribution and long-term survival in a heavily polluted sediment core from the Bay of Bagnoli (Tyrrhenian Sea, Italy). *Mediterranean Marine Science*, 26(1), 40–54. <https://doi.org/10.12681/mms.37946>

Diatom distribution and long-term survival in a heavily polluted sediment core from the Bay of Bagnoli (Tyrrhenian Sea, Italy)

Angela PELUSI^{1,2}, María Lorena ROMERO MARTÍNEZ^{1,3}, Apurva MULE⁴, Eleonora SCALCO⁴, Ines BARRENECHEA ANGELES^{5,6}, Roberta PIREDDA¹, Wiebe H.C. F. KOOISTRA¹, Marina MONTRESOR¹ and Diana SARNO^{4,7}

¹ Integrative Marine Ecology Department, Stazione Zoologica Anton Dohrn, Villa Comunale, 80121 Napoli, Italy

² Oceanography Section, National Institute of Oceanography and Applied Geophysics, Trieste, Italy

³ Ecosystems, British Antarctic Survey, High Cross, Madingley Road, Cambridge, England, CB3 0ET, United Kingdom

⁴ Department of Research Infrastructures for Marine Biological Resources, Stazione Zoologica Anton Dohrn, Villa Comunale, 80121 Napoli, Italy

⁵ Department of Earth Sciences, University of Geneva, 13, rue des Maraîchers, 1205 Geneva, Switzerland

⁶ Department of Geosciences, UiT-The Arctic University of Norway, Tromsø, Norway

⁷ NBFC, National Biodiversity Future Center, Piazza Marina 61, 90133 Palermo, Italy

Corresponding author: Diana SARNO; diana.sarno@szn.it

Contributing Editor: Stelios SOMARAKIS

Received: 30 May 2024; Accepted: 30 November 2024; Published online: 08 January 2025

Abstract

Diatom resting stages can remain viable in sediments for decades and germinate when exposed to suitable environmental conditions, inoculating the water column and the surface sediments with new populations of cells. Classical methods, based on acid-cleaning of diatom frustules in sediment samples, do not discriminate between living and dead cells and may destroy the more fragile taxa. We used a metabarcoding dataset based on the V9 region of the 18S rRNA (20,602 reads, 102 diatom Amplicon Sequence Variants (ASV)) coupled with the Serial Dilution Culture method to assess diversity and viability of resting stages in a heavily polluted sediment core from the Bay of Bagnoli (Tyrrhenian Sea) spanning approximately two centuries. Our results indicate that planktonic centric diatoms dominated the sediment layers, but ASVs of benthic pennates were also present, especially in older layers. High densities (up to $\sim 2 \cdot 10^6$ cells g^{-1} wet sediment) of viable cells were recorded in the surface layer (dated to 2013) for *Nanofrustulum shiloi* and for a small unidentified pennate diatom. Concentrations of living cells decreased towards older layers, but cultures of *Chaetoceros curvisetus* were still generated from a layer dated to 1954. Selected strains were characterized morphologically, in light and electron microscopy, and molecularly, confirming the records of *N. shiloi*, *Psammogramma* sp. and *Plagiogramma* sp. The results of our study highlight the capability of several centric and pennate diatom species to ‘rest’ alive in severely polluted sediments for decades. This calls for future studies aimed at understanding the mechanisms that regulate dormancy and the adaptation to harsh environmental conditions, which have potential biotechnological applications.

Keywords: Diatoms; Bay of Bagnoli; metabarcoding; resting stages; sediment core; resting stage germination; taxonomy.

Abbreviations: ASV: Amplicon Sequence Variant; eDNA: environmental DNA; SDC: Serial Dilution Culture; LM: Light Microscopy; EM: Electron Microscopy.

Introduction

Many species of microalgae are capable of producing resting stages, which can survive buried in sediments and resume growth once incubated at favourable environmental conditions. Examples are diatom spores and resting cells (McQuoid *et al.*, 2002; Härnström *et al.*, 2011), dinoflagellate cysts (Lundholm *et al.*, 2011; Kremp *et al.*, 2018) and cyanobacterial akinetes (Legrand *et al.*, 2019; Wood *et al.*, 2021). Many diatoms – predominantly cen-

tric planktonic taxa - are known to form physiologically and morphologically differentiated resting stages, called spores. Others can form resting cells, which are morphologically indistinguishable from vegetative cells but have the capability of surviving conditions unsuitable for growth, e.g., low temperatures or darkness (Ellegaard & Ribeiro, 2018). Both centric and pennate diatoms have been reported to produce resting stages (McQuoid and Hobson, 1996), but information on the survival capability of pennate taxa is extremely scanty. The long-term per-

sistence of alive resting stages in undisturbed sediment layers represents an archive of historical populations, and allows tracking changes in their population genetic structure over time and their adaptations to environmental changes (Hattich *et al.*, 2024).

Surface sediments integrate the signal of the planktonic microalgae sinking to the bottom at the end of their growth season with that of the benthic ones living in sediments of coastal areas. Information on the taxonomic composition of microalgal assemblages in sediment samples is challenging and requires specific methods for concentrating cells and separating them from sediment grains. An alternative approach is provided by their DNA signature obtained by the amplification and sequencing of specific barcode regions from environmental DNA (eDNA). The DNA signature of unicellular organisms can be preserved in sediments for up to thousands of years (Ellegaard *et al.* 2020) and metabarcoding approaches enable obtaining temporal datasets to reconstruct the dynamics of natural communities and their response to environmental changes and anthropogenic disturbances (e.g., Capo *et al.*, 2019; Keck *et al.*, 2020; Siano *et al.*, 2021; Barrenechea Angeles *et al.*, 2023). Metabarcoding approaches have been successfully applied to study natural diatom populations in sediment cores collected in marine and freshwater sites at different latitudes (e.g., Zimmermann *et al.*, 2021; Anslan *et al.*, 2022; Singh *et al.*, 2024). This technique has the potential to detect the whole diatom community, including rare species, small and fragile species that do not preserve well, and cryptic species that share very similar morphological characters and are thus difficult to study via traditional light microscopy techniques. The resulting taxonomic coverage is thus much higher, only constrained by the marker of choice and the availability of reference sequences (van der Loos & Nijkand, 2021). Metabarcoding approaches are less time-consuming than microscopy, and potentially allow unbiased comparisons between sites, thus facilitating monitoring programs over large temporal and spatial scales (Pawlowski *et al.*, 2022).

A sediment core spanning ca. two centuries was collected in the Bay of Bagnoli (Gulf of Pozzuoli, Mediterranean Sea, Italy), a heavily polluted industrial area north of the city of Naples, declared Site of National Interest (SIN) in 2000 (Law 388/2000). The sediments contained very high concentrations of heavy metals and polycyclic aromatic hydrocarbons (PAHs) due to now discontinued industrial activities (production of steel, asbestos and cement) and the disposal of contaminated soil close to the coast (Armiento *et al.*, 2020; Armiento *et al.*, 2022; Barrenechea Angeles *et al.*, 2023). PAH concentration at the peak of the industrial activity (1950-1992) was comprised between 144 and 301 mg kg⁻¹ and average concentrations of heavy metals - Cd, Cu, Hg, Pb, and Zn - were above regulatory limits (see Armiento *et al.*, 2022).

A metabarcoding study of eDNA samples (Barrenechea Angeles *et al.*, 2023) allowed reconstructing the temporal dynamic of biological communities - from bacteria to metazoa - highlighting the dominance of the seagrass *Posidonia oceanica* in the oldest layers (1832-

1851), which persisted until the beginning of industrial activities in 1911. The signature of unicellular eukaryotes gradually replaced the plant e-DNA and metazoan sequences dominated the assemblage in the most recent layers, from 2007 to 2013.

Here we focus on the diatom community of the Bagnoli sediment core. Changes in the species composition over time, inferred from the V9 rRNA barcoding marker, were coupled with an assessment of the survival capability of diatom resting stages in the polluted sediments by means of the Serial Dilution Culture (SDC) method (Andersen & Thronsen, 2003). The latter provides an estimate - the Most Probable Number - of alive cells in sediment samples. We expected to find changes in the diatom community composition between the pre-industrial period and the period with the highest pollution loads and we hypothesized that species forming heavily silicified resting spores would dominate in the most polluted sediment layers.

Materials and Methods

Sediment core collection and sed-DNA analysis

A 110 cm long sediment core was collected at 55 m water depth in the Bay of Bagnoli (Gulf of Pozzuoli, Tyrrhenian Sea; 40.8025° N, 14.1486° E; Fig. S1) on December 5th, 2018, with an SW-104 corer Carma®, equipped with a liner of 10.4 cm in diameter. The core was dated and processed as illustrated in Barrenechea Angeles *et al.* (2023). For each of the 20 sediment layers considered in this study, i.e. from 2013 down to 1822 (Figs S2a, b), DNA was extracted from 5 g of sediment using the DNeasy® PowerMax® Soil kit (QIAGEN®, Düsseldorf, Germany) following the manufacturer's instructions. Eukaryotes were targeted by amplifying the V9 region of 18S rRNA (~150 bp) with 1389F -1510R primers (Amaral-Zettler *et al.*, 2009). Sequencing and data processing to obtain ASVs were carried out as described in Barrenechea Angeles *et al.* (2023). ASVs assigned to diatoms were recovered and a new taxonomic assignment was performed using standalone blast in the blast + suite (Camacho *et al.*, 2009) with the newest version of PR2 database version 5.0.0 (Guillou *et al.*, 2012) integrated with private reference sequences from diatom strains collected in the region. Taxonomic assignment was manually curated by further blast in NCBI and notes are reported in the Supplementary data file. We kept the assignments with similarity ≥ 90%, and a query coverage > 90 bp. For the analyses conducted at species and genus levels, the dataset was restricted to ASVs showing similarity with the reference ≥ 95% and with total abundance of reads ≥ 3. The most ancient sample (corresponding to 1822) was excluded from the analyses due to the very low number of total reads (n = 29).

Alpha-diversity was explored using several descriptors, including Richness (Observed ASVs), Chao1 and Shannon index, generated using the R package phyloseq (McMurdie & Holmes, 2013). The Non-metric Multi-

dimensional Scaling analysis (NMDS) was performed based on a Bray-Curtis dissimilarity matrix, using sequences with 90% similarity to the reference database; bar plots and heatmaps were plotted using *microeco* (Liu, *et al.* 2021) and *ggplot2* (Wickham, 2016) R packages.

Quantification of alive diatom resting stages

The concentration of alive diatoms in 12 sediment layers, from 2013 down to 1911, was assessed using a modified version of the SDC method (Andersen & Thronsen, 2003; Montresor *et al.*, 2013). A portion of sediment (Fig. S2b) was collected with a sterile spatula and placed in an airtight plastic bag that was stored in a black bag at 4 °C. Serial dilution experiments were performed within 4 months from sediment collection. One gram (wet weight) of sediment was transferred into a 15 ml Falcon tube containing 9 ml of f/4 medium (sea water: f/2 in a 1:1 ratio) to make the first dilution step (1:10) (Fig. S2c). The Falcon tube was gently shaken until all particles of sediment were thoroughly dispersed in the medium. A 24-well culture plate was filled with 1.8 ml f/4 medium and 200 µl of sample from the first dilution were transferred into each of the first 6 wells (row A) to make up the second dilution step ($0.2 \cdot 10^{-1}$). From the sixth well of row A, 200 µl of sample was used to inoculate the 6 wells of the following row (row B). This procedure was repeated for rows C and D creating four dilution steps. The well-plates were sealed with parafilm and placed at a temperature of 20 °C, under a combination of natural and artificial light regime (12L:12D) provided by cool white fluorescent tubes. Plates were covered with a neutral screen and incubated at an irradiance of $\sim 10 \mu\text{mol photons m}^{-2} \text{s}^{-1}$ for one week, followed by two weeks at $\sim 50 \mu\text{mol photons m}^{-2} \text{s}^{-1}$ irradiance. Plates were inspected once every week, using an inverted microscope (Leica DMIL LED, Leica Microsystems, Wetzlar-Germany). Diatom cells were identified to the species or genus level; several pennate diatoms were classified based on their size and shape.

Ultrastructure and molecular characterization of selected strain of benthic diatoms

To improve the identification of pennate diatoms, a number of clonal cultures were established and prepared for ultrastructural analysis in electron microscopy. Individual cells were isolated from the Serial Dilution Cultures with a sterile drawn Pasteur pipette and placed into a 12 well culture plate containing f/4 medium; plates were incubated at a 12:12 h dark:light photocycle at a temperature of 20 °C. Micrographs of cells that germinated in the SDC and of the isolated strains were taken with an Axiophot light microscope (Carl Zeiss, Oberkochen, Germany) equipped with a Zeiss Axiocam digital camera. For transmission and scanning electron microscopy (TEM and SEM) observations, clean diatom frustules were obtained after removal of the organic matter with

nitric and sulfuric acids and prepared as illustrated in (Sarno *et al.*, 2005). Samples were observed with a JEOL JSM-6500F SEM (JEOL-USA Inc., Peabody, MA, USA) and with a Philips 400 TEM (Philips Electron Optics BV, Eindhoven, Netherlands). Unfortunately, due to the lack of access to the lab during the COVID pandemic, several strains were lost.

For the isolated strains, the DNA barcode was generated by sequencing of V4 region of 18S rRNA. This region was selected since many 18S reference sequences available in GenBank lack part or all of the V9 region, thus impairing their use for taxonomic assignment of V9 barcode data. Genomic DNA was extracted with a CTAB extraction protocol as described in Gaonkar *et al.* (2018). PCR amplification was performed using the primers Ch-300F 5'-ATTAGGGTTTGATTCCGGAGAGG-3' (Gaonkar *et al.*, 2018) and the 1147R 5'-AGTTTCAGCCTTGCGAC-CATAC-3' (Alverson *et al.*, 2007) producing PCR products of approximately 550 bp. The PCR reaction mixture (25 µl in MilliQ water) contained 0.4 µM of each primer, 200 µM of each dNTP, 0.25 µl of Xtra Taq Polymerase and 5 µl 5x Xtra buffer (GeneSpin, Milano, Italy), and 20-70 ng of DNA. PCR was conducted as follows: initial denaturation at 95 °C for 2 min, 35 cycles at 95 °C for 20 s, annealing at 56 °C for 30 s and extension at 72 °C for 1 min, and a final extension at 72 °C for 7 min. PCR products were visualised using low melting agarose TAE (Tris-acetate-EDTA) buffer gel electrophoresis and purified using DNA Isolation Spin Kit Agarose (PanReac Applichem GmbH, Darmstadt, Germany) following manufacturer's instructions. Resulting products were then sequenced with a BigDye Terminator Cycle Sequencing technology (Applied Biosystems, Foster City, CA, USA), purified using a 'Biomek FX' (Beckman Coulter, Fullerton, CA, USA) robotic station, and analysed on an Automated Capillary Electrophoresis Sequencer '3730 DNA Analyzer' (Applied Biosystems). Forward and reverse sequences were combined into contigs and aligned using BioEdit v7.0.0 (Hall, 1999). Any site showing an ambiguity in the forward and reverse sequence was recorded as such, if the surrounding sites read without difficulties.

Results

Metabarcoding

A total of 102 diatom ASVs assigned to diatom reference sequences with similarity $\geq 90\%$, corresponding to 20,602 reads, were retrieved from the total eukaryote dataset included in Barrenechea Angeles *et al.* (2023). (Supplementary data). These ASVs were found to belong to a total of 23 genera and 44 species. The Non-metric Multidimensional Scaling analysis (NMDS, Fig. 1) revealed the presence of a temporal gradient grouping diatom communities of the recent period (including the samples from 1967 to 2013) clearly separated from those in the oldest samples (1842 - 1911), while differences between samples from the intermediate (1921 - 1954) and old periods were more nuanced. The three alpha diversity inde-

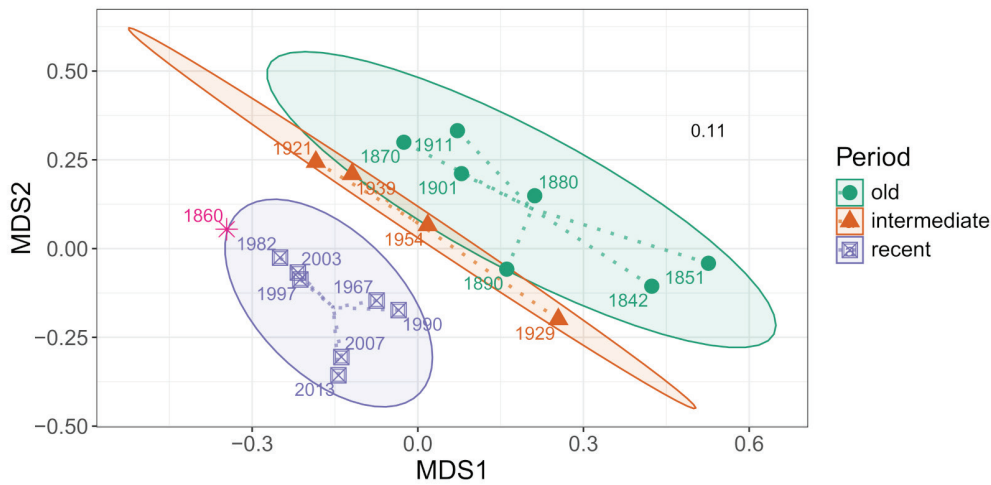


Fig. 1: Non-metric Multidimensional Scaling (NMDS) of sediment samples of core AB01 based on Bray-Curtis dissimilarity matrix (stress=0.11). All points belonging to the same cluster/period were linked to their group centroid with line segments and enclosed by an ellipse. Sample from 1860 (pink) is an outlier of the old period.

ces (Richness, Chao index and Shannon index) showed that diversity was higher in the most recent periods and then decreased in the older ones (Fig. S3).

To identify taxa that characterized the diatom community through time, we selected from the taxonomically curated dataset the 87 ASVs assigned to reference sequences with similarity $\geq 95\%$ (Supplementary data; Fig. 2). The most recent samples (1967 to 2013) showed high relative abundances of centric planktonic diatoms belonging to the genera *Chaetoceros*, *Skeletonema* and *Thalassiosira* together with the tychoplanktonic *Neobrightwellia*, which was represented by the species *Neobrightwellia alternans* (valid new name of *Biddulphia alternans*, (Sims *et al.*, 2023)). However, the temporal trends among genera were different: *Chaetoceros* showed the highest relative abundances in the samples corresponding to the old and intermediate periods ($> 50\%$ of the total reads in the

period 1954-1842), while *Neobrightwellia* was mainly detected in the most recent samples ($>20\%$ in the period 2013-1967 and in 1860). *Skeletonema* ($>10\%$ in the period 2013-2003 and in 1890) and *Thalassiosira* ($\geq 4\%$ in the period 2013-1954) were recorded in almost all layers, but their relative abundance was slightly higher in the most recent ones. ASVs assigned to the benthic araphid genus *Nanofrustulum* showed high abundance percentages in several old layers (generally $>10\%$ in the period 1911-1851) but also in the four most recent ones ($\geq 7\%$ in the period 2013-1997), while percentages were lower in the intermediate period.

Most ASVs of the planktonic genera *Chaetoceros*, *Skeletonema* and *Thalassiosira* could be attributed at the species level with similarity values between 98 and 100% (Supplementary data, Fig. S4). ASVs of *Chaetoceros socialis* and *C. curvisetus 1* (Gaonkar *et al.*, 2018)

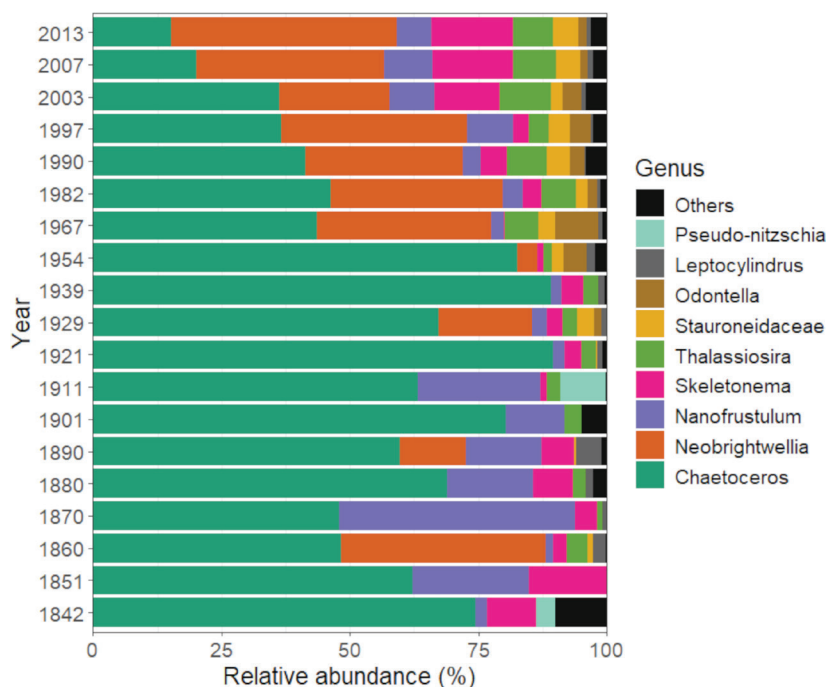


Fig. 2: Relative abundance of the most abundant diatom genera or families recorded in the sediment layers of core AB01.

were the most abundant of their genus; *Skeletonema* was mainly represented by ASVs of *S. menzelii* and *S. pseudocostatum*. The ASVs annotated as *Thalassiosira* sp. 1 matched at 100% with a private sequence of a small *Thalassiosira* (strain C2-A1) isolated from surface sediments collected at LTER-MC on February 2014, whose description as a new species is in progress.

The manual curation of the taxonomic assignment highlighted, in several cases, that the V9 region exhibited low discrimination power at species or even genus level. Indeed, a single ASV could be attributed to more than one taxon with identical similarity values (Supplementary data). A case was represented by the 20 ASVs matching with high similarity values (99.2-100%) to *N. shiloi* and to ‘endosymbiotic Fragilariales diatoms isolated from Foraminifera’; we assigned these ASVs to cf. *N. shiloi*. In cases in which the ASVs were assigned to species belonging to different genera, the ASVs were assigned to the higher common taxonomic rank, i.e., family. These were the cases of ASVs assigned to: i) *Craticula pseudocitrus* (a freshwater diatom) and different species of *Stauroneis*, which we assigned to Stauroneidaceae; and ii) *Eolimnia* and *Sellaphora* cf. *seminulum*, which we assigned to Sellaphoraceae. After the manual curation the total number of genera and species was reduced to 18 and 37, respectively, plus 4 taxa identified only at the family level.

Serial Dilution Cultures

We tested the presence of alive diatom resting stages in twelve sediment layers from 1911 to 2013 with the Serial Dilution Culture method. Alive vegetative cells were detected in the four most recent layers up to a depth of 8 cm, corresponding to the year 1997 (Table 1, Fig. 3). No germination was observed in the older layers, with the exception of the 16 cm depth (dated to 1954), where only *C. curvisetus* was detected with concentrations of $3 \cdot 10^3$ cells \cdot g⁻¹ of wet sediment. A marked quantitative difference was observed between the most recent layer (dated to 2013), where cell density of $\sim 2 \cdot 10^6$ cells \cdot g⁻¹ wet sediment was estimated, and the older layers where alive diatom abundances were considerably lower (Table 1). The two most abundant taxa recorded in the 2013 layer were a small (cell width < 5 μ m), chain-forming diatom identified as cf. *Nanofrustulum* sp. (Fig. 3A) and a very small benthic pennate diatom (pennate sp. 2, probably a *Nitzschia*) that we failed to bring in culture (Fig. 3C); the estimated cell concentration of the two taxa were $>10^6$ and $3.2 \cdot 10^4$ cells \cdot g⁻¹ of wet sediment, respectively.

Chaetoceros socialis (Fig. 3K) and *C. curvisetus* (Fig. 3G) were the most abundant species of this genus, represented also by *C. protuberans* (Fig. 3H), *C. constrictus* (Fig. 3I), and *C. diadema* (Fig. 3J). Very small taxa at

Table 1. Most Probable Number (MPN) of alive diatom taxa (cells \cdot g⁻¹ of wet sediment) recorded with the SDC method in the sediment layers of core AB01. Pictures of a selection of taxa are provided in Figure 3.

Layer depth:	2 cm	4 cm	6 cm	8 cm	16 cm
Layer age:	2013	2007	2003	1997	1954
Cf. <i>Nanofrustulum</i> sp.	1200000				
Pennate diatom sp. 2	460000	13000	1000		
<i>Chaetoceros socialis</i>	65000	5500			
<i>Chaetoceros curvisetus</i>	32000	7000		8500	3050
<i>Thalassiosira</i> sp. 1	35000	7000	900		
Colonial benthic diatom square cells	32000				
Undetermined small (< 10 μ m) pennates	23500	2250		1000	
Colonial benthic diatom elongate cells	7500	16500		1000	
Pennate diatom sp. 3	11000	13000			
Biddulphoid diatom	3900	17000	1000		
<i>Odontotella aurita</i>	13500		2000		
Undetermined large (> 10 μ m) pennates	11500	2250			
Pennate diatom sp. 1	10500				
<i>Thalassiosira</i> sp. 2	8500				
<i>Skeletonema</i> cf. <i>pseudocostatum</i>		1000		3900	
<i>Chaetoceros diadema</i>	3400				
<i>Asterionellopsis</i> sp.	1850	900			
<i>Chaetoceros protuberans</i>	2250				
Cf. <i>Melosira</i>		1000	1000		
<i>Chaetoceros constrictus</i>	900	900			

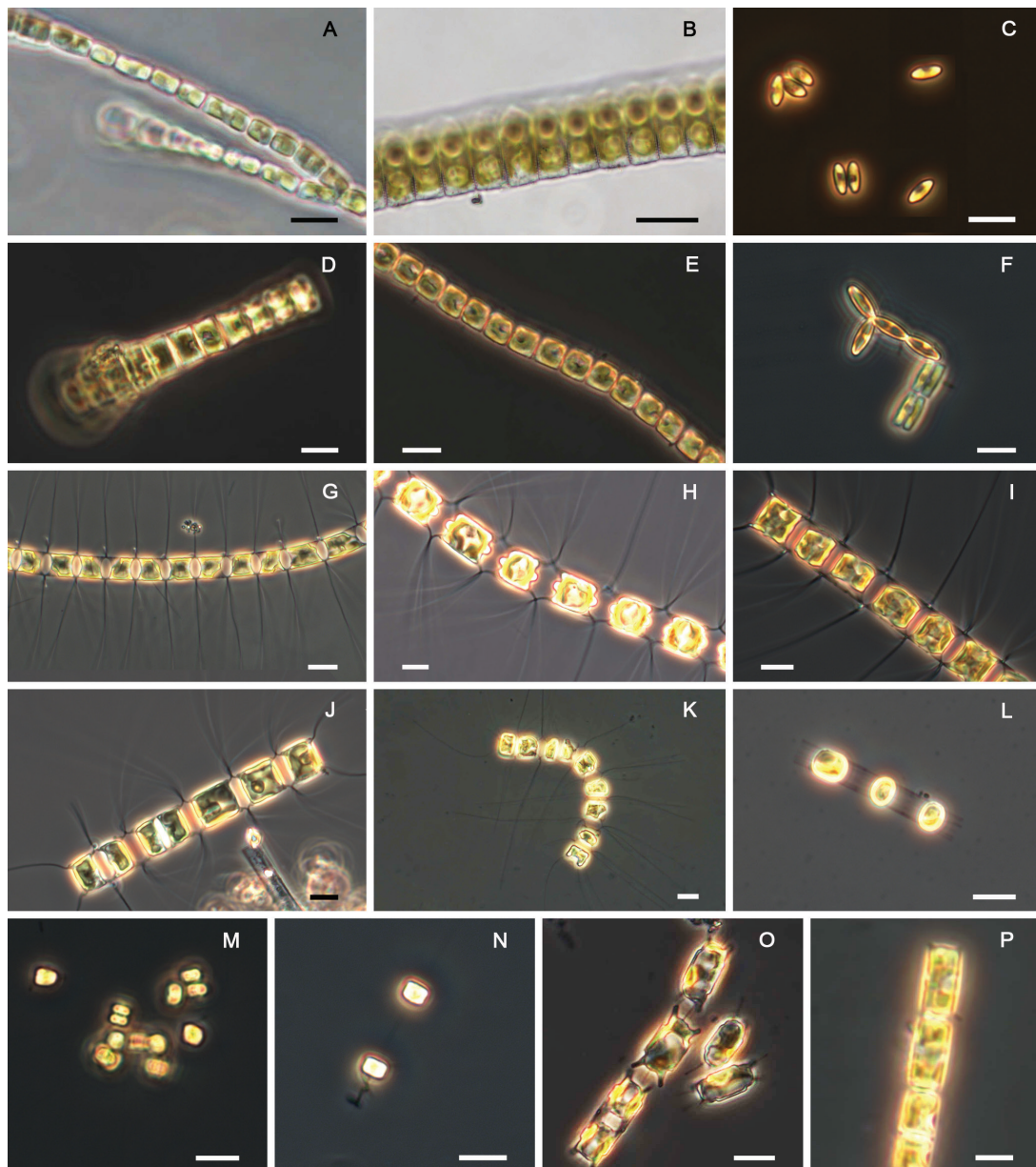


Fig. 3: Light micrographs of diatom taxa recorded from serial dilution cultures. Cf. *Nanofrustulum* sp. (A). Colonial benthic diatom elongate cells (B). Pennate diatom sp. 2 (C). Colonial benthic diatom square cells (D, E). Pennate diatom sp. 3 (F). *Chaetoceros curvisetus* (G). *Chaetoceros protuberans* (H). *Chaetoceros constrictus* (I). *Chaetoceros diadema* (J). *Chaetoceros socialis* (K). *Skeletonema* cf. *pseudocostatum* (L). *Thalassiosira* sp. 1 (M). *Thalassiosira* sp. 2 (N). *Odontella aurita* (O). Biddulphioid diatom (P). Scale bars = 20 μm (B, G); 10 μm (A, C-J, L-O); 5 μm (K, P).

tributed to the genus *Thalassiosira* were also abundant: a solitary species (*Thalassiosira* sp. 1) (Fig. 3M) and a morphotype forming short chains (*Thalassiosira* sp. 2) (Fig. 3N). The genus *Skeletonema* was represented by *S.* cf. *pseudocostatum* (Fig. 3L). Taxa identified in light microscopy as *Odontella aurita* (Fig. 3O) were detected together with smaller colonial biddulphioid diatoms, loosely defined as bipolar centric taxa with elevated apices with pseudocells (Sims et al 2023), (Fig. 3P); unfortunately cultures of both species/morphotypes were lost. Two benthic diatoms forming ribbon chains were relatively abundant in different sediment layers: they were distinguished by the shape of cells and were identified as “colonial benthic diatom elongate cells” (Fig. 3B) and “colonial benthic diatom square cells” (Figs 3D, E). Finally, unidentified pennate diatoms were placed in two

categories based on their size because it was impossible to identify them even at the genus level in light microscopy (e.g., Fig. 3C, F).

Frustule ultrastructure and barcodes of selected diatom strains

With the aim to improve the identification of taxa detected in the SDCs, we established clonal cultures of some pennate benthic diatoms and in the following we illustrate their morphology and ultrastructure and provide partial 18S rRNA reference sequences, which include the V4 region.

Nanofrustulum shiloi (J.J.Lee, Reimer & McEnery) Round, Hallsteinsen & Paasche

Class: Bacillariophyceae; Order: Fragilariales; Family: Staurosiraceae; Genus: *Nanofrustulum*

Strains examined: BD9, LR13, LR26, (LR21 only for morphology)

Molecular characterization: Partial 18S sequences: GenBank Accession numbers PP808715, PP808714, PP808716, respectively. Note: the sequences contain a short insertion of an unknown nature.

References: Sar & Sunesen, 2003; Li *et al.*, 2018.

Cylindrical cells forming chains (Fig. 4A) linked by interlocking marginal spines (Fig. 4B). Circular valves 2.4 – 3 µm in diameter. Valve surface flat or slightly domed, mantle curved or vertical (Fig. 4B). Central elongate sternum (Figs 4B, C) in some cases not well defined. Uniseriate striae, ~25–30 in 10 µm, each consisting of radial to elongate areolae of size decreasing gradually from valve margin to central sternum. Areolae with branching cribra (Fig. 4C), also present on the valve mantle (Fig. 4D). Valve face with small warts or spines (not shown). Apical pore field present at both apices, both composed of a single small pore (Fig. 4D). Marginal spines positioned on the striae near the junction of the valve and mantle (Fig. 4B), variable in shape and length. Girdle bands are plain, without perforations, valvocopulae consisting of two segments and copulae composed by a series of scale-like segments (not shown).

The partial 18S rRNA gene sequences were within 99% similarity of *N. shiloi* strain CCMP1306 (GeneBank accession number: MF093126) and a distance tree of BLAST results resolved these sequences in a clade with other sequences of this species. The identification of several strains as *N. shiloi* supports the abundance of this species in the sediment core as suggested by metabarcoding data and the observations of the SDC material in light microscopy (Table 1).

***Psammogramma* sp.**

Class: Bacillariophyceae; Order: Plagiogrammales; Family: Plagiogrammaceae; Genus: *Psammogramma* S. Sato et Medlin

Strains examined: BD2, BD4, BD11

Molecular characterization: Partial 18S sequences: GenBank Accession numbers PP808717, PP808718 and PP808719, respectively.

Reference: Sato *et al.*, 2008; Li *et al.*, 2020.

Cells attached in chains by valve faces (Figs 4E, F). Valves linear-elliptical (Figs 4G, H) to elliptical (Fig. 4I), tending to become round (Figs 4J, K) when they reduce their size. Valves 2.7–15 µm long and 2.7–3.0 µm wide. Barely visible sternum (Figs 4G-I). Transapical striae uniseriate and parallel throughout along the indistinct sternum (20–22 in 10 µm) (Figs 4G-I). Round areolae occluded by fine rotae (Fig. 4L). Short projections, granules or spinules, on the valve face-mantle junction (Figs 4I-K). Well-developed apical pore fields (Figs 4H, J) sometimes ornamented externally with silica granules around and between the pores (Fig. 4J). Internally, apical pore fields plain and composed of several vertical rows of small pores (Fig. 4L) Girdle composed by open and unperforated bands (Figs 4H, J).

The genus *Psammogramma* includes only two species, *P. vigoensis* and *P. anacarae*. The two species can be distinguished by the presence of linear valves in *P. anacarae* vs. linear-elliptical valves in *P. vigoensis*, alternating striae in *P. vigoensis* vs. parallel striae in *P. anacarae* and the occasional presence of spines near the apices in *P. vigoensis*. Our strains resemble but are not identical to *P. vigoensis*.

The partial 18S rRNA gene sequences of strains BD4 and BD11 were within 98% similarity of those of *Neofragilaria nicobarica* and *N. montgomeryii*, and only within 97% similarity of that of *P. vigoensis*, the only 18S sequence of this genus available in GenBank. A distance tree of BLAST results resolved the sequences in a clade with those of *Neofragilaria* and *Psammogramma*, but not particularly close to any of these. The sequence of strain BD2 was very short, and BLAST results inconclusive. The cells identified as “colonial benthic diatoms elongate cells” in serial dilution cultures may correspond to species of the genus *Psammogramma*.

***Plagiogramma* sp.**

Class: Bacillariophyceae; Order: Plagiogrammales; Family: Plagiogrammaceae; Genus: *Plagiogramma* Greville, amend Chunlian Li, Ashworth & Witkowski

Strain examined: BD15

Molecular characterization: Partial 18S sequence: GenBank accession number PP808720

Reference: Li *et al.*, 2020.

Cells attached in chain by valve faces (Figs 4M, N). Valves elliptical (Fig. 4P), about 27 µm long, 8 µm wide, with 7 striae in 10 µm. Striae uniseriate and continuous on the mantle, containing round areolae. Cribra not visible, probably destroyed by the cleaning. Sternum centrally expanded (Figure 4P). Valve face-mantle junction bearing siliceous spines externally (Fig. 4N, O). Apical pore fields extending from the valve face onto the mantle. Apical pore fields with minute granules externally (Fig. 4O) and plain internally (Fig. 4Q). Valvocopula plain and wider than copulae. Copulae narrow and perforated by a single row of pores (Fig. 4N). Based on these morphological features the strain BD15 belongs to the *Plagiogramma-Dimeregramma* complex proposed by (Li *et al.*, 2020). These authors suggested that there is no evidence to keep *Plagiogramma* and *Dimeregramma* as separate genera and proposed merging *Dimeregramma* with *Plagiogramma*, because the latter has the priority.

The partial 18S rRNA gene sequence of strain BD15 exhibited 99.7% similarity with the one of *Dimeregramma* sp. strain HK377 (GenBank accession number KF701597). Cells identified as “colonial benthic diatoms square cells” in serial dilution cultures may correspond to species of the genus *Plagiogramma*.

***Nitzschia adhaerens* Mucko & Bosak**

Class: Bacillariophyceae; Order: Bacillariales; Family: Bacillariaceae; Genus: *Nitzschia*

Strain examined: LR40

Molecular characterization: Partial 18S sequence: GenBank accession number PP808721.

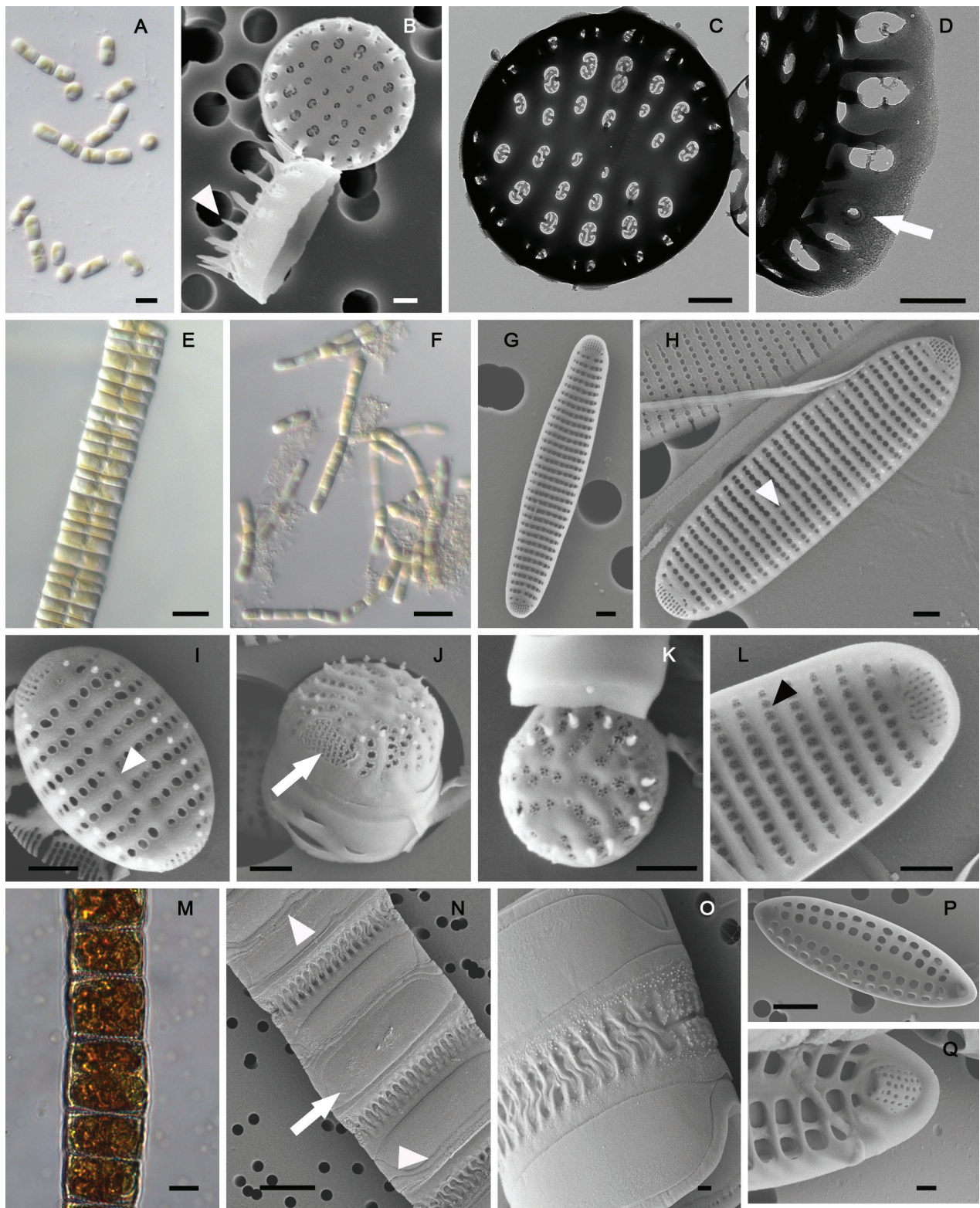


Fig. 4: Micrographs of diatom strains: LM (A, E-F, M); SEM (B, G-L, N-Q); TEM (C-D). *Nanofrustulum shiloi* (A-D); strains: LR26 (A, D), LR21 (B-C). Cells in chains (A). Valves in valve view and in girdle view with marginal spines arrowhead (B). Valve with central sternum, uniseriate striae and areolae with branching cribra (C). Detail of the valve mantle with the single apical pore arrowed (D). *Psammogramma* sp. (E-L); strains: BD2 (F, K); BD4 (E, G-H, L); BD11 (I-J). Chains of larger (E) and smaller (F) cells. Internal view of the valve with uniseriate striae and apical pore fields (G). External view of linear (H) and elliptical (I) valve with the central sternum (arrowhead). External view of round valves with spinules on the valve face-mantle junction and ornamented apical pore (arrow) (J-K). Detail of the internal view of a valve showing the apical pore field and the round areolae occluded by fine rotae (arrowhead) (L). *Plagiogramma* sp. (M-Q, strain BD15). Cells in chain (M). External view of a chain showing the wide and plain valvocopula (arrow) and the narrow copulae perforated by a single row of pores (arrowhead) (N). Detail of the frustule, showing the siliceous spines and the apical pore fields with minute granules (O). Internal view of the elliptical valve (P). Detail of the internal view of a valve showing the apical pore field (Q). Scale bars = 10 μm (E-F, M-N), 5 μm (A, P), 1 μm (G-L, O, Q), 0.5 μm (B-D).

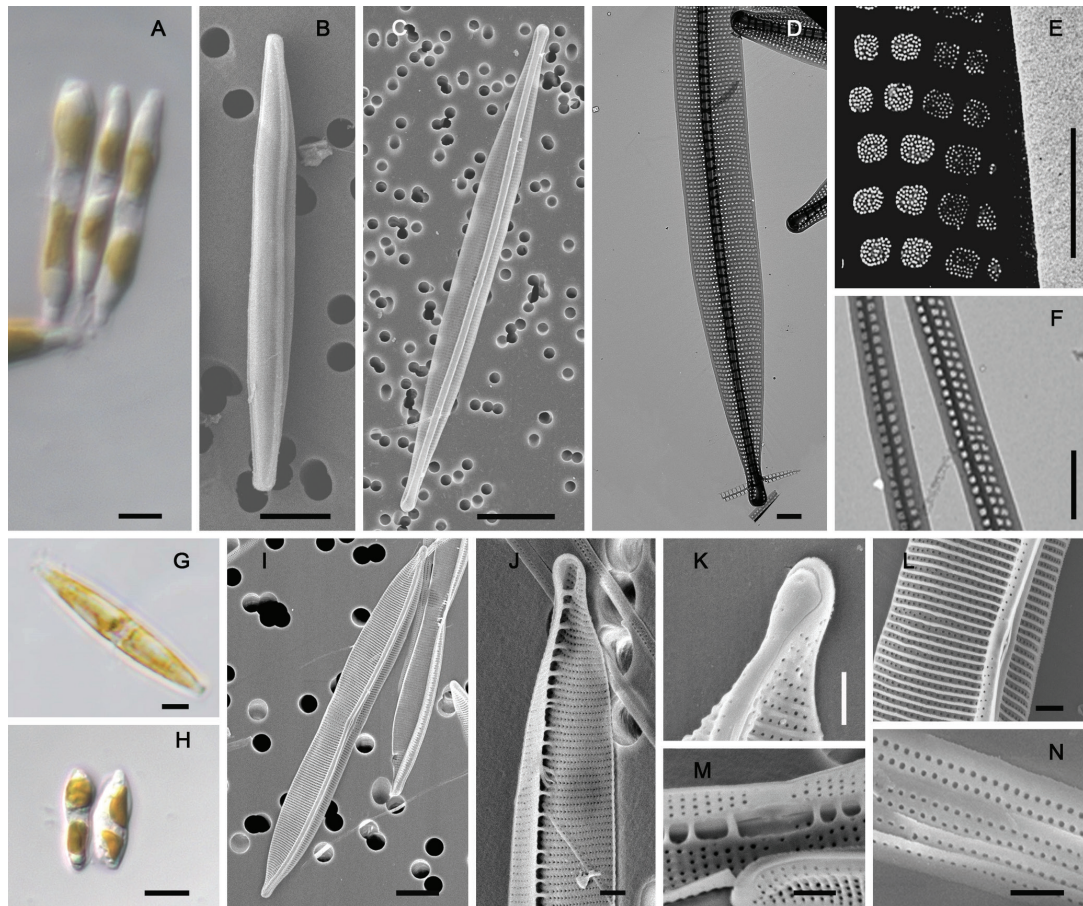


Fig. 5: Micrographs of diatom strains: LM (A, G-H); SEM (B-C; I-N); TEM (D-F). *Nitzschia adhaerens* (A-F, strain LR40). Group of cells with two chloroplasts (A). Lanceolate cell (B). External view of a valve with the slightly eccentric raphe (C). Part of a valve showing the raphe with fibulae and lacking a central nodule (D). Detail of a valve with round areolae occluded by finely perforated hymens (E). Detail of girdle bands with two or three rows of round pores (F). *Nitzschia traheaformis* (G-N); strains LR43 (H), NAMC3 (L, N), PN11 (G, I-M). Cells with two chloroplasts (G-H). External view of a valve with a central constriction on the raphe side (I). Detail of the internal view of a valve showing fibulae and uniseriate striae (J). Detail of the external view of a valve showing the hooked terminal end (K). External view of the valve showing central nodule and canal raphe with 1-2 rows of poroids. Note that striae are composed by a single row of areolae located in shallow grooves (L). Internal view of the raphe with fibulae and central nodule (M). Detail of girdle bands with 1 or 2 rows of round poroids (N). Scale bars = 10 μm (G-H), 5 μm (A-C, I), 1 μm (D, F, J-N), 0.5 μm (E).

Reference: Mucko *et al.*, 2021.

Cells with two chloroplasts (Fig. 5A). Valves lanceolate, 27–34 μm long and 2.5–3 μm wide (Figs 5B, C). Raphe slightly eccentric/almost central, without a central nodule (Figs 5C, D). Relatively dense and regularly spaced fibulae (23–24 in 10 μm) (Fig. 5D). Uniseriate striae (47–58 in 10 μm) composed of tiny round to rectangular areolae (Fig. 5D); areolae (ca 6 in 1 μm) occluded by finely perforated hymens (Fig. 5E). Valvocopula open, with two or three rows of round pores enclosed by finely perforated hymens (Fig. 5F).

Results of a Blast search with the partial 18S of strain LR40 showed 100% identity with that of *N. adhaerens* isolate BIOTAI-60 (GenBank accession number MH734167), one of the strains of this species in the original species description. The morphological and molecular data show that strain LR40 belongs to *N. adhaerens*.

Nitzschia traheaformis Chunlian Li, Witkowski & Yu
Class: Bacillariophyceae; Order: Bacillariales; Family:

Bacillariaceae; Genus: *Nitzschia*

Strains examined LR43, NAMC3, PN11 (this strain was isolated in Portonovo along the Adriatic coast of Italy).

Reference: Witkowski *et al.*, 2016.

Molecular characterization: Partial 18S sequence: GenBank accession numbers PP808722, PP808723 and PP808724, respectively.

Cells with two chloroplasts (Figs 5G-H). Linear-lanceolate valves, 22–48 μm long and 3.8–6 μm wide with cuneate, slightly capitate apices (Figs 5G, I). Valves constricted in the centre on the raphe side where the opposite side is nearly straight. Raphe strongly eccentric with a central nodule (Figs 5I, J, M, L) and hooked terminal ends (Fig. 5K). Canal raphe with 1 or 2 rows of relatively large poroids (Fig. 5L). Fibulae (15–17 in 10 μm) form simple arches bridging the two sides of valves (Fig. 5J). Uniseriate striae (31–32 in 10 μm) composed of circular areolae (ca 5 in 1 μm) located in shallow grooves (Fig. 5L). Girdle bands open with 1 or 2 rows of round poroids (Fig. 5N).

The partial 18S rRNA gene sequences of strains LR43,

NAMC3 and PN11 were identical to that of the type material of *N. traheaformis*, i.e., strain SZCZCH971 (GenBank accession number KT943643). Morphological and molecular data fit the original description of the species.

Discussion

The results of our metabarcoding study show a diverse assemblage of diatom ASVs in the sediment core collected in the Bay of Bagnoli, in spite of the high levels of contamination by heavy metals and toxic organic compounds both at the surface (Sprovieri *et al.*, 2020) and in the deeper layers (Armiento *et al.*, 2022; Barrenechea Angeles *et al.*, 2023). ASVs attributed to centric planktonic diatoms were dominant, but pennate benthic taxa were represented particularly in the deeper layers. As expected, the structure of the diatom community was different in the period with the highest pollution level (from 1950 to the present) as compared to the older, less impacted layers. The SDC experiments show that not all these ASVs represent cells able to resume growth when exposed to favourable conditions. A considerable fraction of alive cells consisted of benthic araphid diatoms difficult to identify at the species or even genus level in light microscopy. Ultrastructural and genetic characterization of strains isolated from SDCs helped at identifying some of these pennate taxa.

Metabarcoding diversity in the sediment core

The V9 universal primers used here for the metabarcoding assessment were designed for amplifying the whole eukaryotic community, including metazoans, higher plants and protists, hence determining a relatively limited number of reads attributed to diatoms (Barrenechea Angeles *et al.*, 2023). Nevertheless, the NMDS clustering generated using only diatom ASVs could resolve distinct assemblages characterizing the pre-industrial period from the most recent polluted ones, confirming the results obtained in a previous study based on a multi-proxy approach of the whole eukaryotic and prokaryotic communities (Barrenechea Angeles *et al.*, 2023). The observed pattern may reflect different DNA preservation, with the most recent layers showing a higher alpha diversity and a more diversified assemblage of diatom genera. The high relative abundance of ASVs attributed to species of the genus *Chaetoceros* may be due to the fact that these species produce heavily silicified spores (Ishii *et al.*, 2011) that may allow a better preservation of the DNA. Sediment samples showed high relative abundances of planktonic genera, such as *Skeletonema* and *Thalassiosira*, capable of forming resting cells, i.e. stages that are morphologically undistinguishable from the vegetative cells, suggesting that also these stages have ultrastructural features that can improve DNA preservation. However, this can be the case also for pennate taxa with different size and level of silicification, which persisted alive for years in polluted sediments. The high percentages of the genera

Chaetoceros, *Thalassiosira* and *Skeletonema*, confirm results obtained with metabarcoding approaches on marine sediments from temperate regions (e.g., Piredda *et al.*, 2018; Dzhenbekova *et al.*, 2018; Liu *et al.*, 2020).

A number of studies on the morphological and genetic diversity of planktonic diatom genera (*Chaetoceros*: Kooistra *et al.*, 2010; Gaonkar *et al.*, 2018; *Skeletonema*: Sarno *et al.*, 2005; Sarno *et al.*, 2007; *Leptocylindrus*: Nanjappa *et al.*, 2013), including strains from our study area, provided curated reference sequences required for an accurate taxonomic assignment of metabarcoding data. Indeed, ASVs of these genera could be assigned at the species level with high similarity values. The most abundant planktonic species recorded in this study – *C. socialis*, *C. curvisetus*, *C. costatus*, *S. pseudocostatum* and *Thalassiosira* sp. 1 - matched those dominating the diatom seed banks at the LTER site MareChiara in the nearby Gulf of Naples (Montresor *et al.*, 2013; Piredda *et al.*, 2017). Relatively high percentages of ASVs assigned with a similarity of 99.1% to *Neobrightwellia alternans* (= *Biddulphia alternans*) were recorded in the most recent sediment layers, i.e., from 1967 onwards. Operational taxonomic units (OTUs) attributed to this species were also recorded in the sediments of the nearby Gulf of Naples (Piredda *et al.*, 2017; Piredda *et al.*, 2018) but this species is not included in the >30 years long dataset of planktonic diatoms, confirming its presence close to the benthic environment. Alive unidentified ‘biddulphioid diatoms’ germinated from different sediment layers suggesting that the diversity of these bipolar centric diatoms is higher than currently known. The molecular signature of pennate diatoms in the V9 metabarcoding dataset was relatively limited; a possible explanation may be the reduced capability of this barcode region to detect pennate diatoms and/or the restricted number of reads in the diatom dataset. 18S-V9 and *rbcL* are the most widely used barcode region for the study of diatoms in freshwater and marine environments and there is some evidence that *rbcL* performs better for the identification of pennate taxa (Rimet *et al.*, 2019; Armbrecht *et al.*, 2022; Turk Dermastia *et al.*, 2023).

The most abundant ASVs of pennate diatoms were those assigned to cf. *N. shiloi*, which is reported from shallow coastal sediments e.g., (Pérez-Burillo *et al.*, 2022) and can be an endosymbiont of benthic foraminifera (Lee, 2011; Prazeres & Renema, 2019). ASV of this species were present in almost all layers of the sediment core and their relative abundance was higher in the pre-industrial period. Its importance was confirmed by the results of the SDC experiment in which this small sized diatom reached very high ‘most probable abundances’ in the surface layer.

The living diversity in the sediment core

To assess if all the different ASVs merely represent extracellular DNA molecules preserved in sediments or actually DNA present in living cells, we applied the SDC method to induce germination of resting stages under ex-

perimental conditions. The SDC method has been applied for different purposes in phycological research: i) for the assessment of diversity and abundance of phytoflagellates in natural water samples (e.g., Haraguchi *et al.*, 2022), ii) to test the success of ballast water treatments by enumerating alive microalgae (Cullen & MacIntyre, 2016), and iii) to estimate the number of alive diatom resting stages in sediment samples (Imai *et al.*, 1984; McQuoid *et al.*, 2002; Montresor *et al.*, 2013). Diatom spores and resting cells are very small with sizes often similar to those of the sand grains; this makes it impossible to recognize them in natural sediment samples. The SDC method provides an indirect assessment, being based on the detection of living vegetative cells that germinate once the sediments are transferred to a fresh culture medium and exposed to light.

It has been suggested that the time elapsing from core slicing can affect survival capability due to the negative impact of the exposure to oxygen and it has been recommended to carry out these experiments within a relatively short time interval (Lundholm *et al.*, 2011). To minimize these effects, we have stored the sediment samples in tightly closed plastic bags in dark and cold conditions and have carried out the germination trials within five months from the slicing of the core. Another important methodological aspect to be considered is to minimize cross contamination between sediment layers. It has been shown that, spiking the core surface with fluorescent microspheres, cross contamination can occur during the retrieval and processing of the sediment cores (Andersson *et al.*, 2023). To minimize these effects, we processed the cores the same day in which they were collected and discarded the outermost portion of the sediment layers to avoid the smear against the liner and possible cross contaminations of the different layers.

A number of studies applying the SDC method to assess diatom viability in sediment samples show that planktonic taxa of centric diatoms producing resting stages represent the largest fraction of the community (e.g., Itakura *et al.*, 1997; McQuoid, 2002; McQuoid *et al.*, 2002; Montresor *et al.*, 2013; Piredda *et al.*, 2017; Andersson *et al.*, 2023), thus supporting the findings of metabarcoding studies. Yet, in the Bay of Bagnoli, benthic diatoms represent the most important fraction of the resurrected diatom population reaching concentrations $>1.5 \cdot 10^6$ cells g^{-1} of wet sediment in the layer dated to 2013 and thousands of cells in older layers. These results demonstrate that also several pennate diatoms can survive in conditions not optimal for growth in a resting state. The diversity and abundance of alive diatoms in sediments depends on the species-specific capability to persist viable in the absence of light and high pollutant concentration, and from differences in the propensity to form resting stages, which is evident when comparing the abundances of vegetative cells in the water column with the number of viable resting stages in the sediments estimated by the SDC method (Montresor *et al.*, 2013).

In studies based on the SDC method, benthic pennate diatom taxa present in sediments are generally identified at the genus level or sorted in groups based on cell size

(e.g. McQuoid, 2002; Montresor *et al.*, 2013; Piredda *et al.*, 2017). This is due to the difficulty of identifying these taxa at the species level when observing full living cells in light microscopy. Cleaning the frustules allows a much better resolution of the ultrastructural characters used for species identification (e.g., Martínez, *et al.*, 2021; Pérez-Burillo *et al.*, 2022), but this method does not provide a quantitative estimate of the different taxa and it does not discriminate between living and dead cells.

The ultrastructural investigation in electron microscopy, coupled with barcoding of a region of 18S rRNA that includes the V4 marker, confirmed the presence of *N. shiloi* as shown by the results of the metabarcoding analysis. This study also suggests that two relatively abundant chain-forming taxa identified as ‘colonial benthic diatom square cells’ and ‘colonial benthic diatom elongate cells’ can be attributed to species of the genera *Dimeregramma* and *Psammogramma*, respectively. The ultrastructural study on culture material also shows that *Psammogramma* presents a broad cell size range and that the smallest cells could be misidentified for *N. shiloi* when examining alive material in light microscopy. Two *Nitzschia* species (*N. traheaformis* and *N. adhaerens*) were also identified thanks to the ultrastructural and molecular characterization, showing that these analyses are required to achieve a better picture of the diversity of benthic pennate diatoms and provide reference sequences for the interpretation of metabarcoding data.

Research perspectives

Besides benthic pennate diatoms, also several planktonic centric taxa – e.g., *Chaetoceros* species, *Odontella aurita*, *Skeletonema pseudocostatum*, two *Thalassiosira* – could be resurrected from polluted sediments dating back ~ 20 years and up to ~ 60 years for the record of *Chaetoceros curvisetus* in 1954. Core AB01 was sampled in front of the old docks of the decommissioned industrial area of Bagnoli; PAH concentration at the peak of the industrial activity (1950-1992) was between 144 and 201 $mg \cdot kg^{-1}$ and average concentrations of heavy metals - Cd, Cu, Hg, Pb, and Zn – were above regulatory limits (Armiento *et al.*, 2022; Barrenechea Angeles *et al.*, 2023). Concentrations of both heavy metals and PAHs in the recent layers, corresponding to the post-industrial years, indicate a persistent contamination. Planktonic taxa spend their growth season in the water column and sink to the bottom at the end of the blooms. Indeed, a study carried out on the planktonic communities of the study area in different seasons did not provide evidence for degraded ecological conditions (Margiotta *et al.*, 2020). In surface sediments, some species transform into resting stages that could persist for longer time thanks to their heavily silicified cell walls, reduced metabolic activity and specific physiological adaptations (Ellegaard & Ribeiro, 2018). Benthic diatoms, however, spend their whole life on the sediments and should have developed specific adaptations to grow and rest in such a hostile environment. Laboratory studies indeed demonstrate that some species have the capabili-

ty to tolerate high concentrations of heavy metals (Mišić Radić *et al.*, 2021; Andersson *et al.*, 2022;) and PAH (Othman *et al.*, 2023). However, these experiments test relatively short-term exposure to contaminants in culture. Our study shows that several benthic taxa have the capability to live and survive for decades in contaminated environments. It will be worth studying the biological basis of these specific adaptations that may be employed for phytoremediation purposes (Marella *et al.*, 2020; Blaginina *et al.*, 2024). Our study also highlights the diversity of diatom resting stages present in marine sediments, from the heavily silicified spores, to the resting cells of both centric and pennate diatoms, which are capable to ‘rest’ alive for years in the dark. The functional mechanisms allowing this long term survival are still completely unknown.

Acknowledgements

This study was supported by the project ABBAco funded by the Italian Ministry for Education, University and Research, grant number C62F16000170001. This study was also supported by the National Recovery and Resilience Plan (NRRP), Mission 4 Component 2 Investment 1.4 - Call for tender No. 3138 of 16 December 2021, rectified by Decree n.3175 of 18 December 2021 of Italian Ministry of University and Research funded by the European Union – NextGenerationEU; Award Number: Project code CN_00000033, Concession Decree No. 1034 of 17 June 2022 adopted by the Italian Ministry of University and Research, CUP D33C22000960007, Project title “National Biodiversity Future Center - NBFC. M.L. Romero Martínez has been supported by a PhD fellowship funded by the Stazione Zoologica Anton Dohrn (Open University – Stazione Zoologica Anton Dohrn PhD Program). A. Mule has been supported by a PhD fellowship co-funded by the Università Politecnica delle Marche and the Stazione Zoologica Anton Dohrn. The authors thank F. Tramontano for culture media preparation; A. Graziano, F. Iamunno for assistance with sample preparation and EM-observation.

References

- Alverson, A.J., Jansen, R.K., Theriot, E.C., 2007. Bridging the Rubicon: Phylogenetic analysis reveals repeated colonizations of marine and fresh waters by thalassiosiroid diatoms. *Molecular Phylogenetics and Evolution*, 45, 193-210.
- Amaral-Zettler, L.A., McCliment, E.A., Ducklow, H.W., Huse, S.M., 2009. A method for studying protistan diversity using massively parallel sequencing of V9 hypervariable regions of small-subunit ribosomal RNA genes. *PLoS ONE*, 4, e6372.
- Andersen, P., Throndsen, J., 2003. Estimating cell numbers. p. 99-129 In: *Manual on Harmful Marine Microalgae*. Hallegraeff, G.M., Anderson, D.M., Cembella, A.D. (Eds). IOC-UNESCO, Paris.
- Andersson, B., Godhe, A., Filipsson, H.L., Zetterholm, L., Edler, L. *et al.*, 2022. Intraspecific variation in metal tolerance modulate competition between two marine diatoms. *The ISME Journal*, 16 (2), 511-520.
- Andersson, B., Rengefors, K., Kourtchenko, O., Johannesson, K., Berglund, O. *et al.*, 2023. Cross-contamination risks in sediment-based resurrection studies of phytoplankton. *Limnology and Oceanography Letters*, 8 (2), 376-384.
- Anslan, S., Kang, W., Dulias, K., Wünnemann, B., Echeverría-Galindo, P. *et al.*, 2022. Compatibility of diatom valve records with sedimentary ancient DNA amplicon data: A case study in a brackish, alkaline Tibetan lake. *Frontiers in Earth Science*, 10, 824656.
- Armbrrecht, L., Weber, M. E., Raymo, M.E., Peck, V.L., Williams, T. *et al.*, 2022. Ancient marine sediment DNA reveals diatom transition in Antarctica. *Nature Communications*, 13 (1), 5787.
- Armiento, G., Caprioli, R., Cerbone, A., Chiavarini, S., Crovato, C. *et al.*, 2020. Current status of coastal sediments contamination in the former industrial area of Bagnoli-Coroglio (Naples, Italy). *Chemistry and Ecology*, 36 (6), 579-597.
- Armiento, G., Barsanti, M., Caprioli, R., Chiavarini, S., Conte, F. *et al.*, 2022. Heavy metal background levels and pollution temporal trend assessment within the marine sediments facing a brownfield area (Gulf of Pozzuoli, Southern Italy). *Environmental Monitoring and Assessment*, 194 (11), 814.
- Barrenechea Angeles, I., Romero-Martínez, M. L., Cavaliere, M., Varrella, S., Francescangeli, F. *et al.*, 2023. Encapsulated in sediments: eDNA deciphers the ecosystem history of one of the most polluted European marine sites. *Environment International*, 172, 107738.
- Blaginina, A., Zheleznova, S., Miroshnichenko, E., Gevorgiz, R., Ryabushko, L., 2024. The Diatom *Nanofrustulum shiloi* As a Promising Species in Modern Biotechnology. *Applied Biochemistry and Microbiology*, 60 (3), 483-495.
- Camacho, C., Coulouris, G., Avagyan, V., Ma, N., Papadopoulos, J. *et al.*, 2009. BLAST+: architecture and applications. *BMC Bioinformatics*, 10 (1), 1-9.
- Capo, E., Rydberg, J., Tolu, J., Domaizon, I., Debros, D. *et al.*, 2019. How Does Environmental Inter-annual Variability Shape Aquatic Microbial Communities? A 40-Year Annual Record of Sedimentary DNA From a Boreal Lake (Nylandssjön, Sweden). *Frontiers in Ecology and Evolution*, 7, 245.
- Cullen, J.J., MacIntyre, H. L., 2016. On the use of the serial dilution culture method to enumerate viable phytoplankton in natural communities of plankton subjected to ballast water treatment. *Journal of Applied Phycology* (28), 279-298.
- Dzhembekova, N., Moncheva, S., Ivanova, P., Slabakova, N., Nagai, S., 2018. Biodiversity of phytoplankton cyst assemblages in surface sediments of the Black Sea based on metabarcoding. *Biotechnology & Biotechnological Equipment*, 32 (6), 1507-1513.
- Ellegaard, M., Ribeiro, S., 2018. The long-term persistence of phytoplankton resting stages in aquatic ‘seed banks’. *Biological Reviews*, 93 (1), 166-183.
- Ellegaard, M., Clokie, M.R.J., Czepionka, T., Frisch, D., Godhe, A. *et al.*, 2020. Dead or alive: sediment DNA archives as tools for tracking aquatic evolution and adaptation. *Communications Biology*, 3 (1), 169.
- Gaonkar, C.C., Piredda, R., Minucci, C., Mann, D.G., Montre-

- sor, M. *et al.*, 2018. Annotated 18S and 28S rDNA reference sequences of taxa in the planktonic diatom family Chaetocerotaceae. *PLoS ONE*, 13 (12), e0208929.
- Guillou, L., Bachar, D., Audic, S., Bass, D., Berney, C. *et al.*, 2012. The Protist Ribosomal Reference database (PR2): a catalog of unicellular eukaryote Small Sub-Unit rRNA sequences with curated taxonomy. *Nucleic Acids Research*, 41 (D1), D597-D604.
- Hall, T.A., 1999. BioEdit: a user-friendly biological sequence alignment editor and analysis program for Windows 95/98/NT. *Nucleic Acids Symposium Series*, 41, 95-98.
- Haraguchi, L., Moestrup, Ø., Jakobsen, H.H., Lundholm, N., 2022. Phytoflagellate diversity in Roskilde Fjord (Denmark), including the description of *Pyramimonas octopora* sp. nov. (Pyramimonadales, Chlorophyta). *Phycologia*, 61 (1) 45-59.
- Härnström, K., Ellegaard, M., Andersen, T.J., Godhe, A., 2011. Hundred years of genetic structure in a sediment revived diatom population. *Proceedings of the National Academy of Sciences of the United States of America*, 108 (10), 4252-4257.
- Hattich, G.S.I., Jokinen, S., Sildever, S., Gareis, M., Heikkinen, J. *et al.*, 2024. Temperature optima of a natural diatom population increases as global warming proceeds. *Nature Climate Change*, 14, 518-525.
- Imai, I., Itoh, K., Anraku, M., 1984. Extinction dilution method for enumeration of dormant cells of red tide organisms in marine sediments. *Bulletin of Plankton Society of Japan*, 31, 123-124.
- Ishii, K.-I., Iwataki, M., Matsuoka, K., Imai, I., 2011. Proposal of identification criteria for resting spores of *Chaetoceros* species (Bacillariophyceae) from a temperate coastal sea. *Phycologia*, 50 (4), 351-362.
- Itakura, S., Imai, I., Itoh, K., 1997. 'Seed bank' of coastal planktonic diatoms in bottom sediments of Hiroshima Bay, Seto Inland Sea, Japan. *Marine Biology*, 128, 497-508.
- Keck, F., Millet, L., Debroas, D., Etienne, D., Galop, D. *et al.*, 2020. Assessing the response of micro-eukaryotic diversity to the Great Acceleration using lake sedimentary DNA. *Nature Communications*, 11 (1), 3831.
- Kooistra, W.H.C.F., Sarno, D., Hernández-Becerril, D.U., Assmy, P., Di Prisco, C. *et al.*, 2010. Comparative molecular and morphological phylogenetic analyses of taxa in the Chaetocerotaceae (Bacillariophyta). *Phycologia*, 5, 471-500.
- Kremp, A., Hinners, J., Klais, R., Leppanen, A.P., Kallio, A., 2018. Patterns of vertical cyst distribution and survival in 100-year-old sediment archives of three spring dinoflagellate species from the Northern Baltic Sea. *European Journal of Phycology*, 53 (2), 135-145.
- Lee, J.J., 2011. Diatoms as endosymbionts. p. 437-464 In: *The Diatom World. Cellular Origin, Life in Extreme Habitats and Astrobiology*. Seckbach, J., Kociolek, P. (Eds). Springer, Dordrecht.
- Legrand, B., Miras, Y., Beauger, A., Dussauze, M., Latour, D., 2019. Akinetes and ancient DNA reveal toxic cyanobacterial recurrences and their potential for resurrection in a 6700-year-old core from a eutrophic lake. *Science of the Total Environment*, 687, 1369-1380.
- Li, C.L., Witkowski, A., Ashworth, M.P., Dąbek, P., Sato, S. *et al.*, 2018. The morphology and molecular phylogenetics of some marine diatom taxa within the Fragilariaceae, including twenty undescribed species and their relationship to *Nannofrustulum*, *Opephora* and *Pseudostaurosira*. *Phytotaxa*, 355 (1), 1-104.
- Li, C., Ashworth, M.P., Mackiewicz, P., Dąbek, P., Witkowski, J. *et al.*, 2020. Morphology, phylogeny, and molecular dating in Plagiogrammaeae family focused on *Plagiogramma-Dimeregramma* complex (Urneidophycidae, Bacillariophyceae). *Molecular Phylogenetics and Evolution*, 148, 106808.
- Liu, L., Wang, Z., Lu, S., 2020. Diversity and geographical distribution of resting stages of eukaryotic algae in the surface sediments from the southern Chinese coastline based on metabarcoding partial 18S rDNA sequences. *Marine Ecology*, 41 (3), e12585.
- Liu, C., Cui, Y., Li, X., Yao, M., 2021. microeco: an R package for data mining in microbial community ecology. *FEMS Microbiology Ecology*, 97 (2), fiaa255.
- Lundholm, N., Ribeiro, S., Andersen, T.J., Koch, T., Godhe, A. *et al.*, 2011. Buried alive - germination of up to a century-old marine protist resting stages. *Phycologia*, 50 (6), 629-640.
- Marella, T.K., López-Pacheco, I.Y., Parra-Saldívar, R., Dixit, S., Tiwari, A., 2020. Wealth from waste: Diatoms as tools for phycoremediation of wastewater and for obtaining value from the biomass. *Science of the Total Environment*, 724, 137960.
- Margiotta, F., Balestra, C., Buondonno, A., Casotti, R., D'Ambra, I. *et al.*, 2020. Do plankton reflect the environmental quality status? The case of a postindustrial Mediterranean bay. *Marine Environmental Research*, 160, 104980.
- Martínez, Y.J., Siqueiros-Beltrones, D.A., Marmolejo-Rodríguez, A.J., 2021. Response of Benthic Diatom Assemblages to Contamination by Metals in a Marine Environment. *Journal of Marine Science and Engineering*, 9 (4), 443.
- McMurdie, P.J., Holmes, S., 2013. phyloseq: an R package for reproducible interactive analysis and graphics of microbiome census data. *PLoS ONE*, 8 (4), e61217.
- McQuoid, M.R., 2002. Pelagic and benthic environmental controls on the spatial distribution of a viable diatom propagule bank on the Swedish west coast. *Journal of Phycology*, 38, 881-893.
- McQuoid, M.R., Godhe, A., Nordberg, K., 2002. Viability of phytoplankton resting stages in the sediments of a coastal Swedish fjord. *European Journal of Phycology*, 37, 191-201.
- McQuoid, M.R., Hobson, L.A., 1996. Diatom resting stages. *Journal of Phycology*, 32 (6).
- Mišić Radić, T., Čačković, A., Penezić, A., Dautović, J., Lončar, J. *et al.*, 2021. Physiological and morphological response of marine diatom *Cylindrotheca closterium* (Bacillariophyceae) exposed to cadmium. *European Journal of Phycology*, 56 (1), 24-36.
- Montresor, M., Di Prisco, C., Sarno, D., Margiotta, F., Zingone, A., 2013. Diversity and germination patterns of diatom resting stages at a coastal Mediterranean site. *Marine Ecology Progress Series*, 484, 79-95.
- Mucko, M., Bosak, S., Mann, D.G., Trobajo, R., Wetzel, C. E. *et al.*, 2021. A polyphasic approach to the study of the genus *Nitzschia* (Bacillariophyta): three new planktonic

- species from the Adriatic Sea. *Journal of Phycology*, 57 (1), 143-159.
- Nanjappa, D., Kooistra, W.H.C.F., Zingone, A., 2013. A reappraisal of the genus *Leptocylindrus* (Bacillariophyta), with the addition of three species and the erection of *Tenuicylindrus* gen. nov. *Journal of Phycology*, 49, 917-936.
- Othman, H.B., Pick, F.R., Hlaili, A.S., Leboulanger, C., 2023. Effects of polycyclic aromatic hydrocarbons on marine and freshwater microalgae—A review. *Journal of Hazardous Materials*, 441, 129869.
- Pawlowski, J., Bruce, K., Panksep, K., Aguirre, F.I., Amalfitano, S. *et al.*, 2022. Environmental DNA metabarcoding for benthic monitoring: A review of sediment sampling and DNA extraction methods. *Science of the Total Environment*, 818, 151783.
- Pérez-Burillo, J., Valoti, G., Witkowski, A., Prado, P., Mann, D.G. *et al.*, 2022. Assessment of marine benthic diatom communities: insights from a combined morphological–metabarcoding approach in Mediterranean shallow coastal waters. *Marine Pollution Bulletin*, 174, 113183.
- Piredda, R., Sarno, D., Lange, C. B., Tomasino, M. P., Zingone, A. *et al.*, 2017. Diatom resting stages in surface sediments: a pilot study comparing Next Generation Sequencing and Serial Dilution Cultures. *Cryptogamie Algologie*, 38, 31-46.
- Piredda, R., Claverie, J.-M., Decelle, J., de Vargas, C., Dunthorn, M. *et al.*, 2018. Diatom diversity through HTS-metabarcoding in coastal European seas. *Scientific Reports*, 8 (1), 18059.
- Prazeres, M., Renema, W., 2019. Evolutionary significance of the microbial assemblages of large benthic Foraminifera. *Biological Reviews*, 94 (3), 828-848.
- Rimet, F., Gusev, E., Kahlert, M., Kelly, M.G., Kulikovskiy, M. *et al.*, 2019. Diat.barcode, an open-access curated barcode library for diatoms. *Scientific Reports*, 9 (1), 15116.
- Sar, E.A., Sunesen, I., 2003. *Nanofrustulum shiloi* (Bacillariophyceae) from the Gulf of San Matías (Argentina): Morphology, distribution and comments about nomenclature. *Nova Hedwigia*, 77 (3-4), 399-406.
- Sarno, D., Kooistra, W.H.C.F., Medlin, L. K., Percopo, I., Zingone, A., 2005. Diversity in the genus *Skeletonema* (Bacillariophyceae). II. An assessment of the taxonomy of *S. costatum*-like species, with the description of four new species. *Journal of Phycology*, 41, 151-176.
- Sarno, D., Kooistra, W.H.C.F., Balzano, S., Hargraves, P. E., Zingone, A., 2007. Diversity in the genus *Skeletonema* (Bacillariophyceae): III. Phylogenetic position and morphological variability of *Skeletonema costatum* and *Skeletonema grevillei*, with the description of *Skeletonema ardens* sp. nov. *Journal of Phycology*, 43, 156-170.
- Sato, S., Kooistra, W.H.C.F., Watanabe, T., Matsumoto, S., Medlin, L.K., 2008. A new araphid diatom genus *Psammoneis* gen. nov. (Plagiogrammaceae, Bacillariophyta) with three new species based on SSU and LSU rDNA sequence data and morphology. *Phycologia*, 47 (5), 510-528.
- Siano, R., Lassudrie, M., Cuzin, P., Briant, N., Loizeau, V. *et al.*, 2021. Sediment archives reveal irreversible shifts in plankton communities after World War II and agricultural pollution. *Current Biology*, 31, 2682–2689.
- Sims, P.A., Ashworth, M.P., Theriot, E.C., Manning, S.R., 2023. Molecular and morphological analysis of *Biddulphia sensu lato*: a new diagnosis of *Biddulphia*, with a description of the new genera *Biddulphiella* and *Neobrightwellia*. *Marine Micropaleontology*, 178, 102186.
- Singh, P., Teixeira, J.C., Bolch, C., Armbrrecht, L., 2024. Marine sedimentary ancient DNA from Antarctic diatoms. *Palaeogeography, Palaeoclimatology, Palaeoecology*, 640, 112090.
- Sprovieri, M., Passaro, S., Ausili, A., Bergamin, L., Finoia, M.G. *et al.*, 2020. Integrated approach of multiple environmental datasets for the assessment of sediment contamination in marine areas affected by long-lasting industrial activity: the case study of Bagnoli (southern Italy). *Journal of Soils and Sediments*, 20 (3), 1692-1705.
- Turk Dermastia, T., Vascotto, I., Francé, J., Stanković, D., Mozetič, P., 2023. Evaluation of the *rbcL* marker for metabarcoding of marine diatoms and inference of population structure of selected genera. *Frontiers in Microbiology*, 14, 1071379.
- van der Loos, L.M., Nijland, R., 2021. Biases in bulk: DNA metabarcoding of marine communities and the methodology involved. *Molecular Ecology*, 30 (13), 3270-3288.
- Wickham, H., 2016. *ggplot2: Elegant Graphics for Data Analysis*. Springer International Publishing Cham, 12 pp.
- Witkowski, A., Li, C., Zgłobicka, I., Yu, S.-X., Ashworth, M. *et al.*, 2016. Multigene assessment of biodiversity of diatom (Bacillariophyceae) assemblages from the littoral zone of the Bohai and Yellow Seas in Yantai Region of Northeast China with some remarks on ubiquitous taxa. *Journal of Coastal Research* (74), 166-195.
- Wood, S.M., Kremp, A., Savelle, H., Akter, S., Varti, V.P. *et al.*, 2021. Cyanobacterial Akinete Distribution, Viability, and Cyanotoxin Records in Sediment Archives From the Northern Baltic Sea. *Frontiers in Microbiology*, 12, 681881.
- Zimmermann, H.H., Stoof-Leichsenring, K.R., Kruse, S., Nürnberg, D., Tiedemann, R. *et al.*, 2021. Sedimentary ancient DNA from the Subarctic North Pacific: how sea ice, salinity, and insolation dynamics have shaped diatom composition and richness over the past 20,000 Years. *Paleoceanography and Paleoclimatology*, 36 (4), e2020PA004091.

Supplementary Data

The following supplementary information is available online for the article:

Fig. S1: Map of the Bay of Pozzuoli (Tyrrhenian Sea, Mediterranean Sea) with the location of the site at which core AB1 was collected (red dot).

Fig. S2: a) Sediment layers of core AB01 on which sedDNA barcoding analysis was carried out. For each layer are indicated: the year (^{210}Pb and ^{226}Ra dating, see (Barrenechea Angeles *et al.*, 2023) and the three periods identified by Multidimensional Scaling

analysis (see Fig. 1). b) Partition of the individual 1-cm sediment layers into subsamples for different biological analyses: protist 1 and 2 for eukaryotic metabarcoding, R for SDC analyses. c) Schematic representation of the Serial Dilution Culture (SDC) setup.

Fig. S3: Estimates of alpha diversity: Richness (Observed ASVs), Chao1 and Shannon index.

Fig. S4: Heat-map illustrating relative abundance of the most abundant diatom ASVs assigned to the species level.

Excel file: Dataset of the ASVs (V9 region of the 18S rRNA) matching at $\geq 90\%$ similarity a diatom reference sequence recorded on 19 sediment layers